

## DYNAMICS OF CONTROLLED BOUNDARY LAYER SEPARATION

Václav Uruba, Martin Knob

Institute of Thermomechanics, AS CR, v. v. i., Praha

### Abstract:

The results of experimental study on a boundary layer separation control are given in the paper. The boundary layer on a flat wall is subjected to adverse pressure gradient. Three control strategies have been chosen for the study, both passive (rough wall, vortex generator) and active (synthetic jet). The separation process is investigated using TR-PIV method. Dynamical aspects of the phenomenon are analyzed in details.

### Experimental setup

The blow-down aerodynamic rig of IT has been used for the experiment. The test section for generation of adverse pressure gradient in channel was designed and manufactured.

In Fig. 1 the schema of experimental setup is shown. The section **A** represents the starting point of adverse pressure gradient region as well as the origin of the streamwise position coordinate  $x$ . The cross-section in **A** position is  $100 \times 100 \text{ mm}^2$ . Downstream of this section, the upper wall is inclined with angle  $\alpha = 16^\circ$ , while the bottom plane wall is used to study the boundary layer separation. To prevent separation from the upper wall, this is permeable and aspirated. The section **B** represents the “mean” position of a boundary layer separation (please note, that the separation point is not stable).

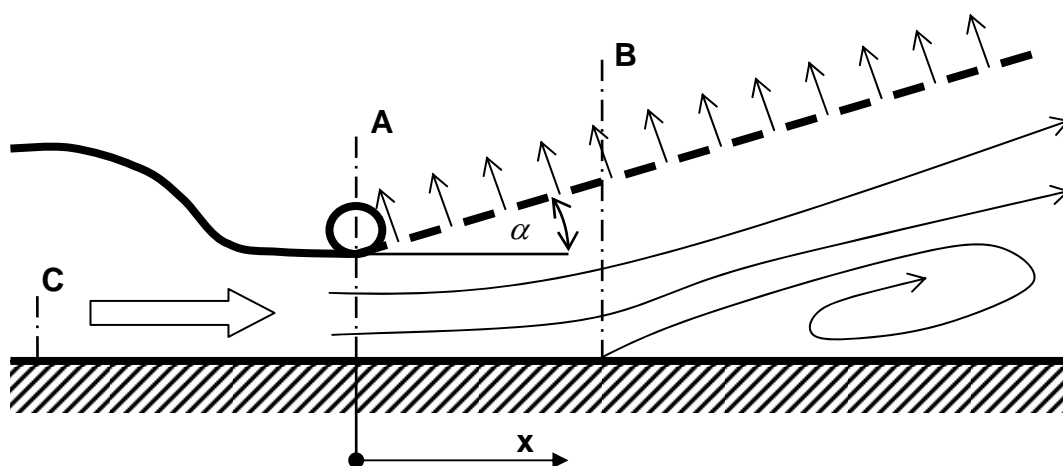


Fig. 1 – Schema of the experimental setup

The mean flow velocity outside boundary layer in section **A** was 12.4 m/s, the boundary layer was of turbulent nature, about 5 mm thick. The suction velocity along the upper wall could be estimated to 5 m/s.

The TR-PIV measuring system DANTEC consists of laser with cylindrical optics and CCD camera. The software FlowMap 3 was used for velocity-fields evaluation. All measurements were carried out in the  $xy$  plane of symmetry. The double-snap acquisition frequency was up to 1.6 kHz.

Detailed description of the experimental setup is given in URUBA, KNOB, POPELKA, 2007.

Three types of flow-control devices are used – wall roughness, vortex generator and synthetic jet (the first two passive, the last active). All control devices were placed near the **A** cross-section.



Fig. 2 – Synthetic jet generator

The wall roughness was simulated by the strip of sand paper No.60, 50 mm in length stuck on the bottom wall, thickness less than 1 mm.

The synthetic jet was fabricated after the NASA design. The slot dimensions  $1.25 \times 35 \text{ mm}^2$ , driven by piezoceramics on cooper membrane dia. 50 mm. Photo of the generator is shown in Fig. 2. The generator has very sharp amplitude-frequency characteristics as shown in Fig. 3 (details see URUBA, 2004). As the

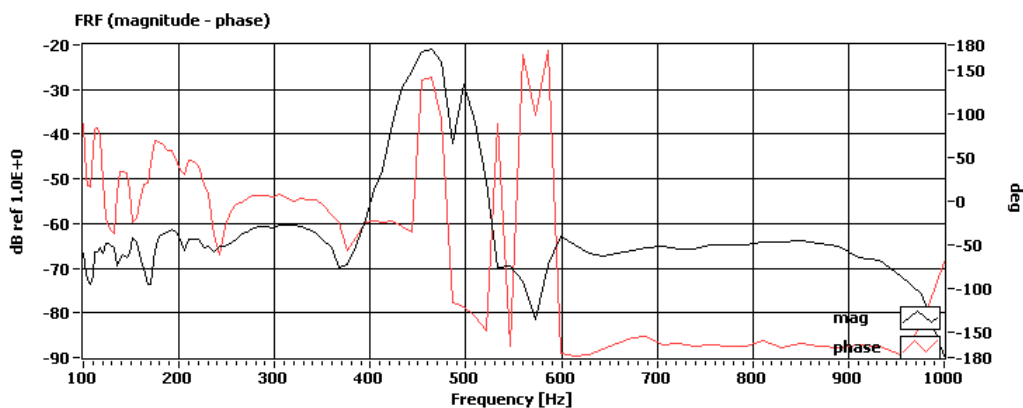


Fig. 3 – Amplitude – frequency characteristic of the synthetic jet

input signal the electrical driving signal is used, while for output of the system the voltage output of the CTA anemometric probe placed near the generator orifice. In Fig. 3 the black line represents relative magnitude (left scale), while red line relative phase (right scale) of the signals.

In control experiments the generator was fed by sinusoidal voltage signal with amplitude 42 V resulting in harmonic flow velocity in the orifice with amplitude approx. 10 m/s in resonance 440 Hz. Design details could be find in CHEN, 2002.

The vortex generator was of the usual type with inclined fences – see Fig. 4.

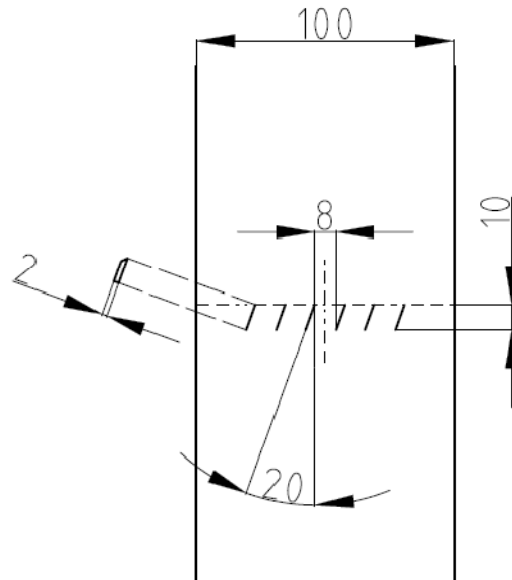


Fig. 4 – Vortex generator

## Results

All diagrams shown hereinafter compare four cases. The first case “Smooth wall” is without control for comparison purpose. Then the “Rough wall”, “Synthetic jet – SJ” and “Vortex generator – VG” are presented showing effectiveness of the 3 control strategies defined above.

The local properties of the boundary layer related to its separation was indicated using the Forward-Flow-Fraction coefficient  $FFF$  defined in URUBA, JONÁŠ, MAZUR, 2007 as a fraction of the time of observation of forward flow direction in a given point. That is for the forward unidirectional flow the  $FFF = 1$  and for backward unidirectional flow  $FFF = 0$ . The  $FFF$  for indication of separation is evaluated near the wall, approx. 1 mm above the wall.

The separation point is defined as the boundary between the forward flow and backward flow of the fluid near the wall, where the stress vanishes. The instantaneous position of the point of separation could be defined as a point in which the streamwise velocity component changes its sign (from positive to negative). The mean position of the point of separation could be evaluated in two ways as a position in which 1) mean streamwise velocity  $U$  near the wall is 0; 2)  $FFF$  near the wall is 0.5.

For evaluation of mean separation characteristics the sets of 1633 vector fields acquired with frequency 500 Hz was used representing 3,2 s of physical time of observation.

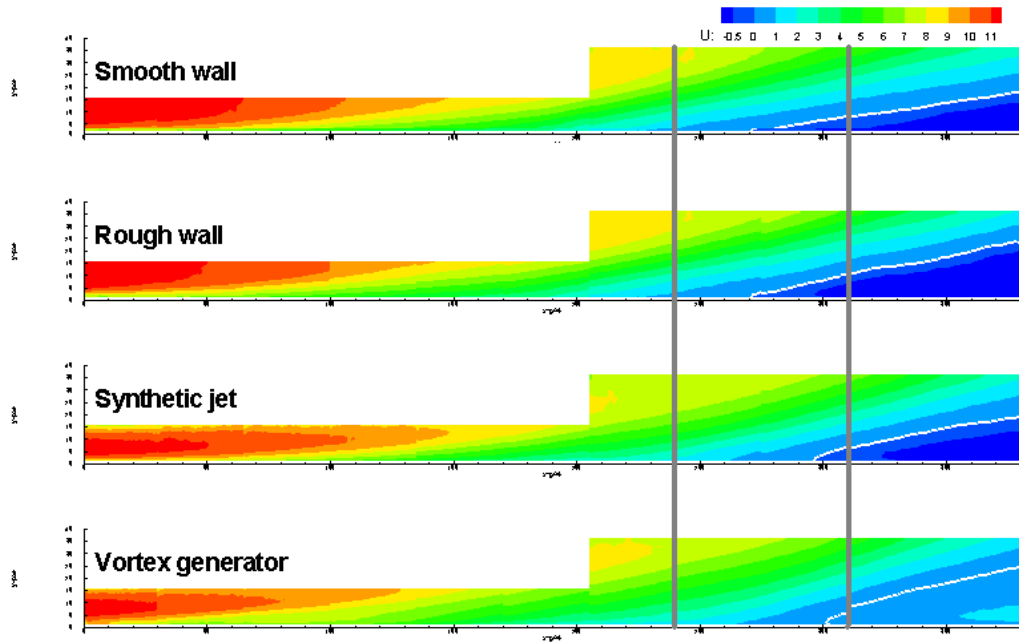


Fig. 5 – Mean streamwise velocity component distribution

In Fig. 5 the distribution of mean streamwise velocity  $U$  near the wall is shown for the 4 cases of interest. The white line in the blue field indicates contour of  $U = 0$ , indicating mean separation point where it touches the wall. The two gray lines delimit the region of further interest  $x \in \langle 240, 310 \rangle$  mm and for  $y = 1$  mm.

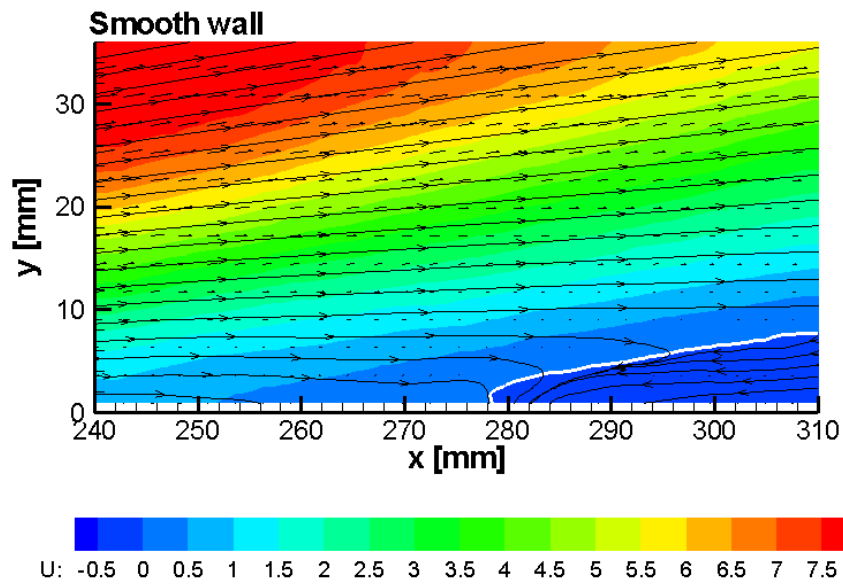


Fig. 6 –  $U$  velocity component distribution with streamlines for smooth wall

Distributions of  $U$  are for all cases similar. Differences could be marked near the position  $x=0$  corresponding to section **A** in Fig. 1, where synthetic jet and vortex generator reduce the velocity gradient resulting in lower velocities. Then, the region in neighborhood of the mean separation point slightly differs too.

Now, let us have a look on the region of interest in details. First of all, in Fig. 6 the detailed distribution of mean streamwise velocity  $U$  for the reference case is shown together with streamlines (more precisely vector lines) calculated from the vector field. The mean recirculation zone is distinct delimited by white line of zero  $U$ .

Then, the comparison of the four cases  $U$  distributions (without streamlines) is shown in Fig. 7.

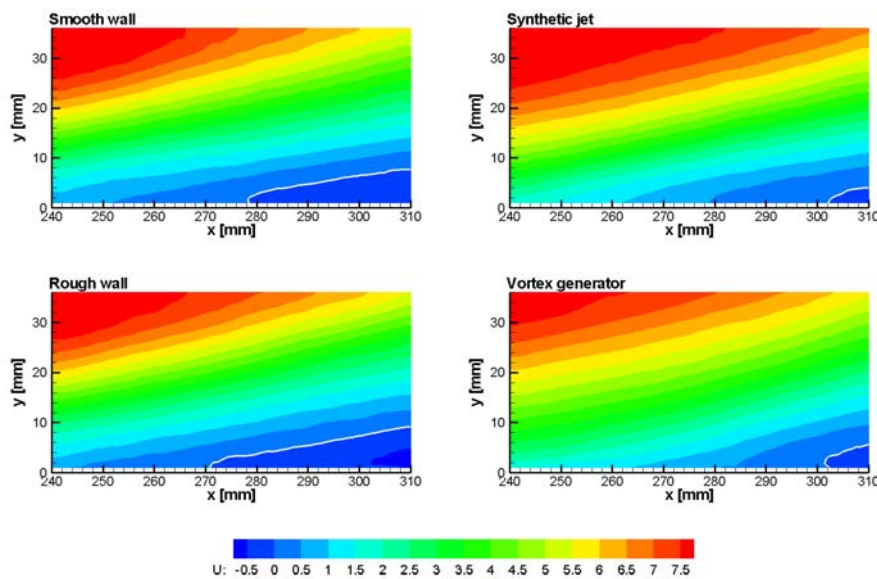


Fig. 7 –  $U$  velocity component distributions

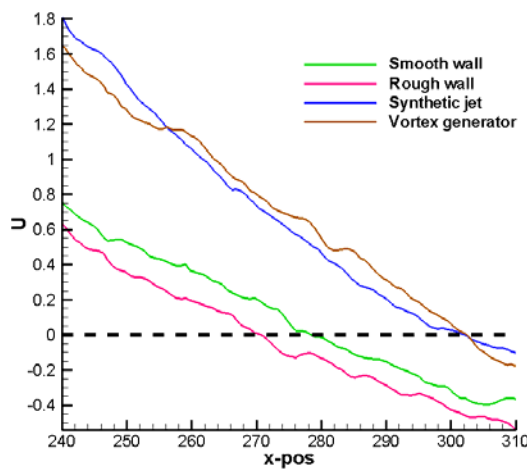


Fig. 8 – Mean streamwise velocity component near the wall

The white line in Fig. 7 shows the position of  $U=0$  enveloping the mean separation region. In Fig. 8 there is the mean streamwise velocity component near the wall (1 mm above) as function of the coordinate  $x$ . The limit value  $U=0$  is represented by the dashed line.

Then, in Fig. 9 the forward-flow-fraction coefficient distributions are shown. The white line represents position  $FFF=0.5$ , while the black line represents  $FFF=0.95$ . In Fig. 10 the courses of forward-flow-fraction coefficient

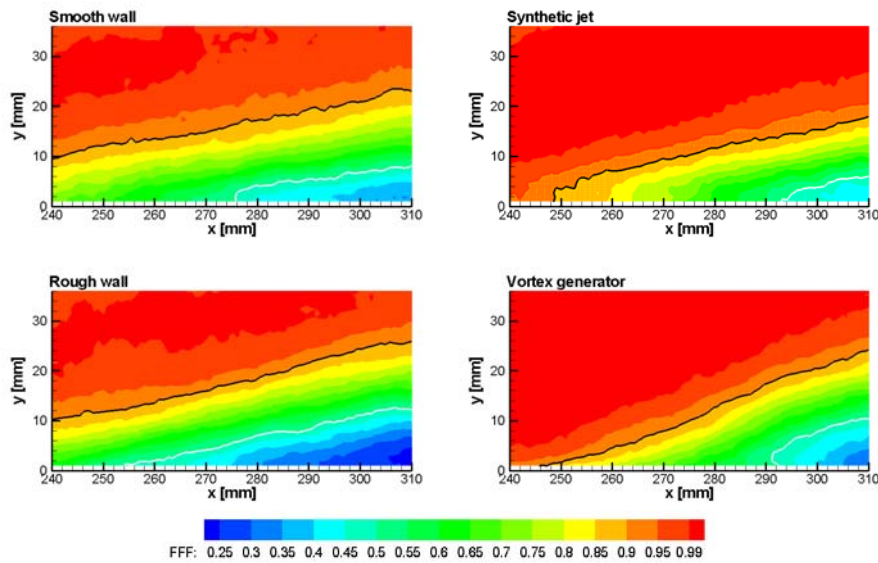


Fig. 9 – *FFF* coefficient distributions

are shown with dashed limit  $FFF = 0.5$ . The mean positions of the point of separation were evaluated using both above given definitions for all cases.

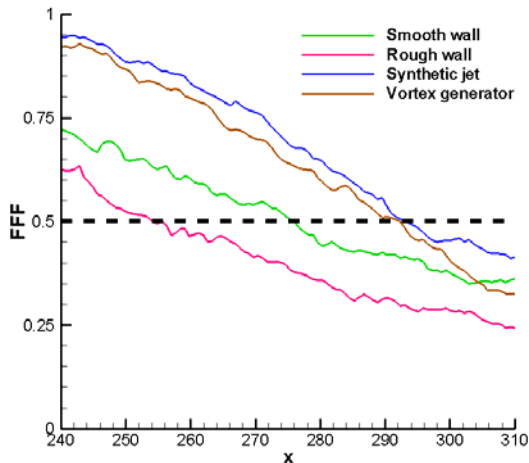


Fig. 10 – Forward-Flow-Fraction coefficient near the wall

The resulting  $x$ -positions in mm are given in Tab. 1. The method using mean streamwise velocity component indicates typically the mean separation point downstream from the position indicated by the forward-flow-fraction coefficient method. The only exception is the comparative smooth wall case, when both methods give exactly the same value.

Obviously, application of the synthetic jet shifted the separation point significantly in the streamwise direction (compare with the smooth wall case), however the vortex generator exhibits almost the same effect. Surprising is the rough wall case, which shows separation even earlier then the smooth wall case. The reason for this behavior is the fact, that the boundary layer is in turbulent state even for the smooth wall and abrupt perturbations excited by the rough wall promote separation.

Tab. 1 – Mean position  $x$  [mm] of the separation point

|                  | $U = 0$ | $FFF = 0.5$ |
|------------------|---------|-------------|
| Smooth wall      | 276     | 276         |
| Rough wall       | 270     | 254         |
| Synthetic jet    | 302     | 292         |
| Vortex generator | 302     | 290         |

Then, other physical quantities have been evaluated, namely variation of the  $U$  and  $V$  velocity components and correlation coefficient of the velocity components.

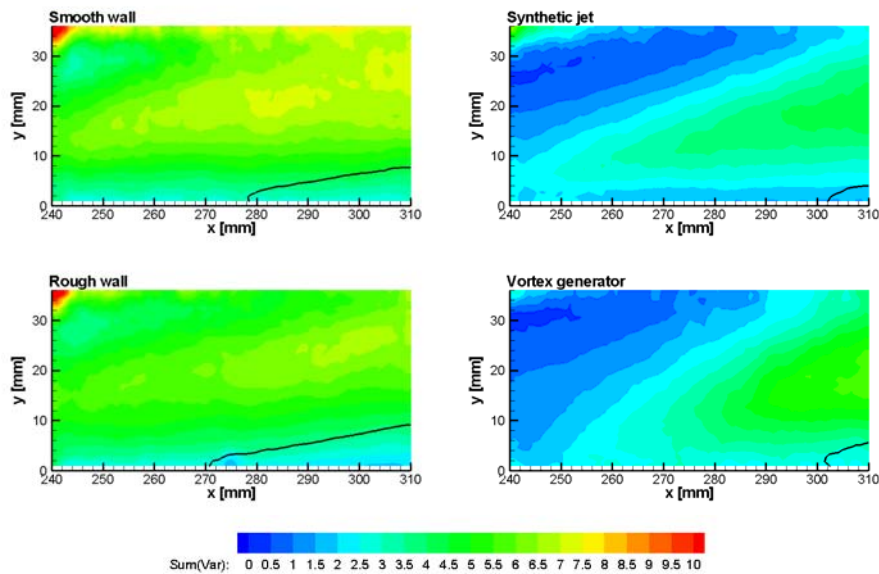


Fig. 11 –  $U$  and  $V$  component variation distributions

The variation of the velocity components indicates fluctuating activity in the flow. The highest level of this activity is found in the zone above the mean separation region, while separation region itself exhibits relatively low activity.

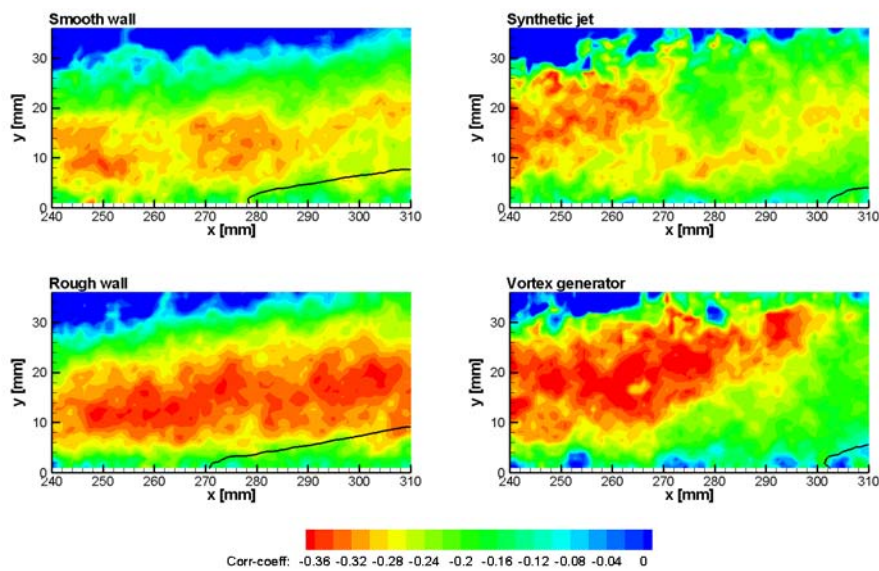


Fig. 12 – Correlation coefficient distributions

Negative value of the correlation coefficient of the longitudinal and transversal velocity components indicates presence of Reynolds stresses, which are connected with

the turbulence production rate. For all configurations the maximum values could be seen above the mean separation region.

The black lines in Figs. 11 and 12 indicates zero  $U$  velocity component – see Fig. 7.

All results shown above indicate that the “smooth wall” and “rough wall” configurations give qualitatively similar results. The same could be stated on “synthetic jet” and “vortex generator” configurations.

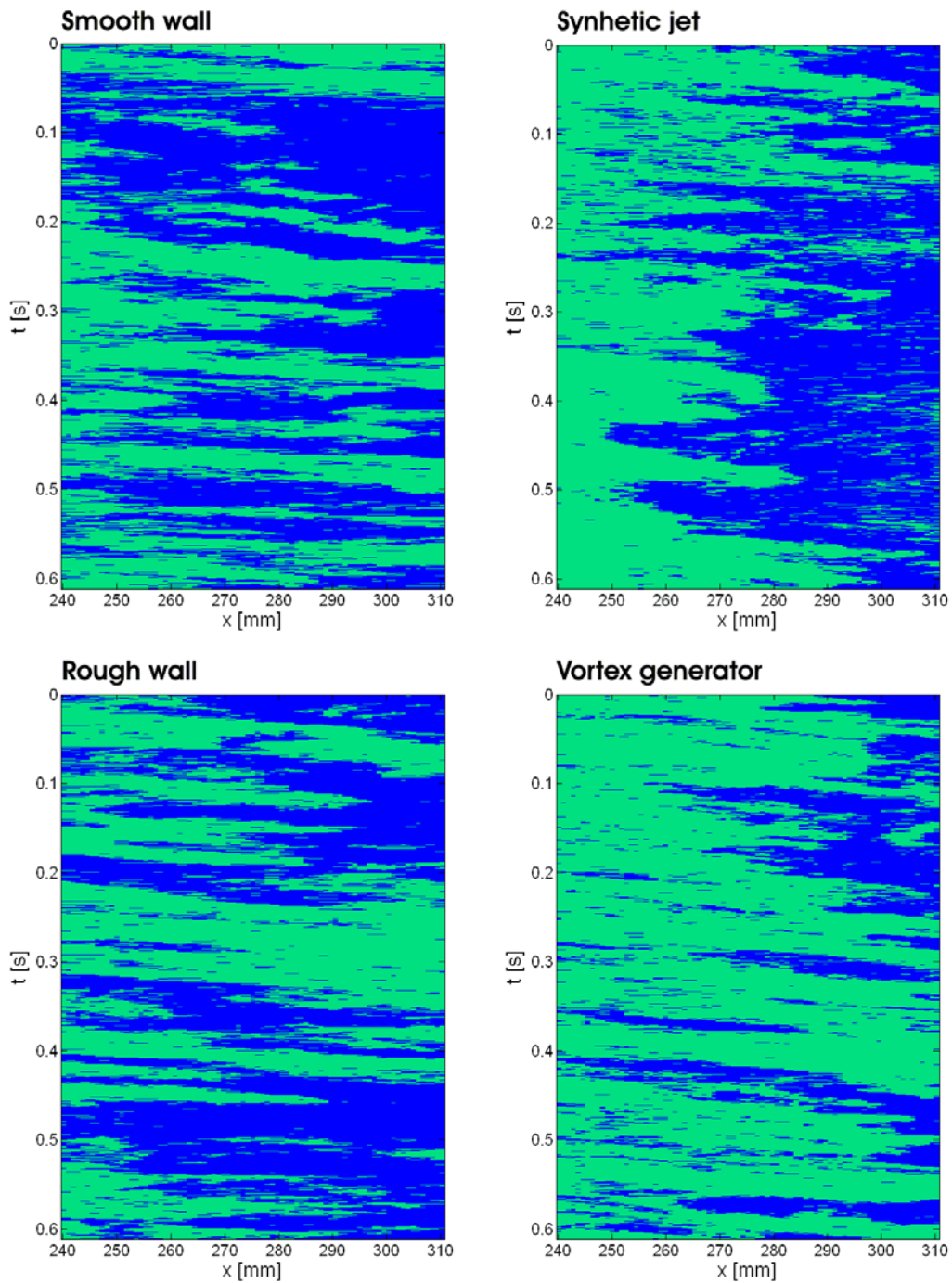


Fig. 13 – Flow direction in the separation region

Now, have a look closer to the dynamics of the separation phenomenon. For this purpose the experiments with higher acquisition frequency have been performed. The frequency was 1633 Hz, while only 1000 subsequent vector maps have been evaluated. Now, the observation period was only 0.6 s. Please note, that this period is not enough for evaluation correct mean values, while the lowest frequencies of the phenomenon are of order 10 Hz. So, the results have shown below are relevant only for the phenomenon dynamics.

Extended region of forward-flow-fraction coefficient values far from both 0 and 1 in Fig. 9 indicates highly dynamical behavior in the near-wall region. To study this dynamics we have evaluated the indicator function time evolution of the region. This function indicates direction of the instantaneous streamwise velocity component in the given point near the wall ( $y = 1$  mm). In Fig. 13 the  $x$  position is on the horizontal axis, while vertical axis represents time  $t$  in seconds. Light green color indicates forward velocity orientation, while blue color indicates backward oriented flow. The first two cases – smooth and rough wall show a lot of blue color with relatively high frequency of changes, pretty regular distribution in time. Similar topology exhibits the synthetic jet actuation with exception that the role of the colors is opposite – now we see more of green indicating forward motion. The last case of vortex generator shows much more irregular, very low frequency behavior indicating occurrence of relative stable streamwise vortices near the wall.

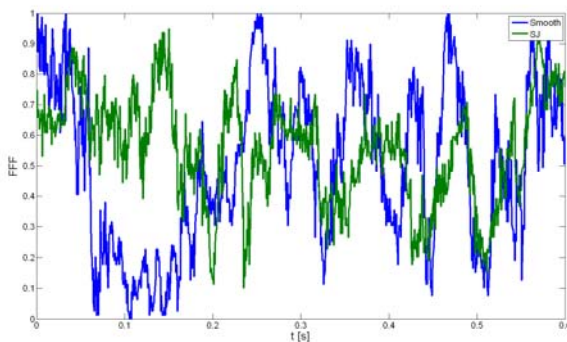


Fig. 14 –  $FFF$  evaluated in whole region in a given moment

Integration of the 2D graphs in Fig. 13 over time obviously gives distribution of the  $FFF$  coefficient (see Fig. 10). To study the time evolution, the integration over  $x$  coordinate has been carried out – see Fig. 14. Only two cases are shown here, blue – smooth wall, green – synthetic jet. Now, the  $FFF = 0$  means backward flow in whole region in a given moment, while  $FFF = 1$  means forward flow in the whole region. Obviously, the synthetic jet configuration exhibits more regular and stable behavior with less fluctuations than smooth wall.

In the Fig. 13 we could recognize color spots indicating time-space regions of forward or backward flow. To study

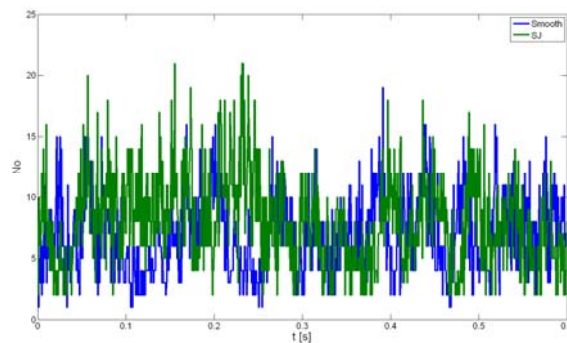


Fig. 15 – Number of regions in a given moment

this structure, we have evaluated number of regions in a given moment – Fig. 15 and mean period of the  $U$  velocity direction changing in a given position – Fig. 16. In Fig. 15 we see time evolution of number of regions in time for smooth wall and

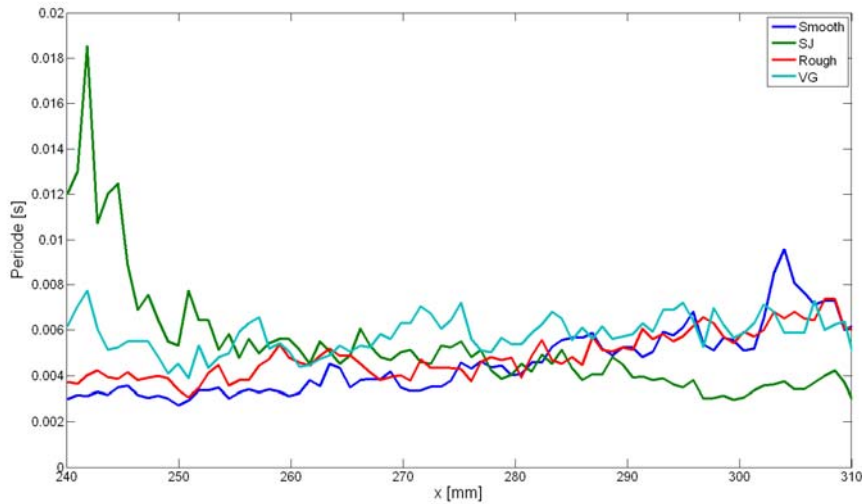


Fig. 16 – Mean period of the  $u$  direction changing

synthetic jet. This number oscillates between 1, corresponding to unbroken region, and 20. The mean period of the  $U$  velocity direction changing in a given position is typically constant or slightly rising along the  $x$  axis, ranging from 3 to 8 ms. But this is not the case of synthetic jet, which shows very high values of periods for low  $x$  and descending tendency.

To complete the dynamical behavior study, the spectra and histograms of the near-wall velocities have been evaluated.

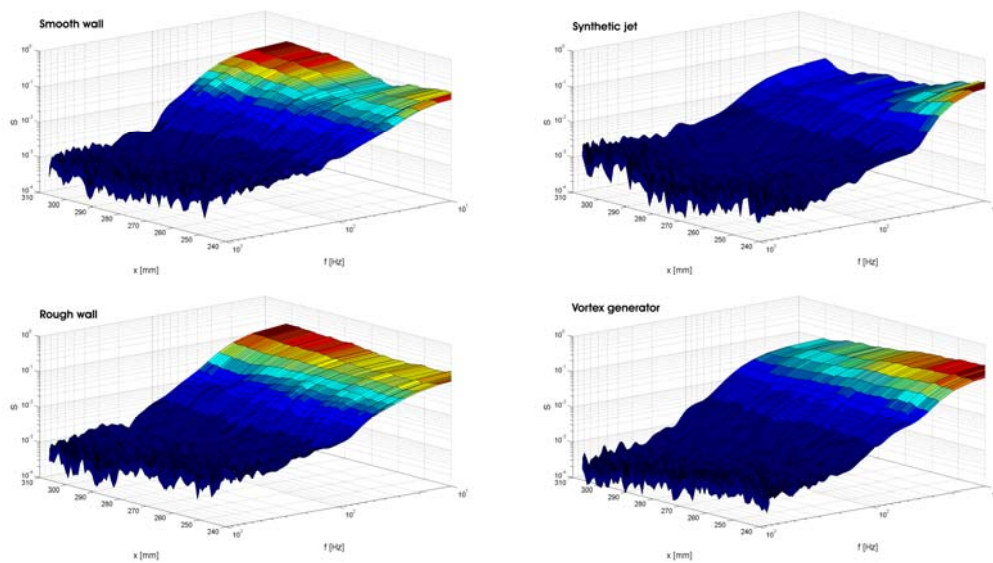


Fig. 17 –  $u$  signal spectra for vortex generator control

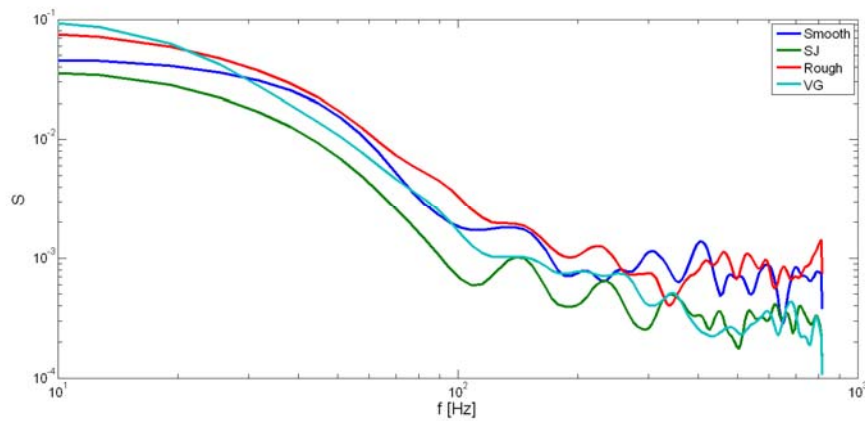


Fig. 18 –  $u$  signal spectra comparison

The spectra for all positions within the zone of interest and for all four cases are shown in Fig. 17, while comparison of the four cases spectra corresponding to the  $x = 270$  mm position is given in Fig. 18. Please note, that both frequency and spectrum

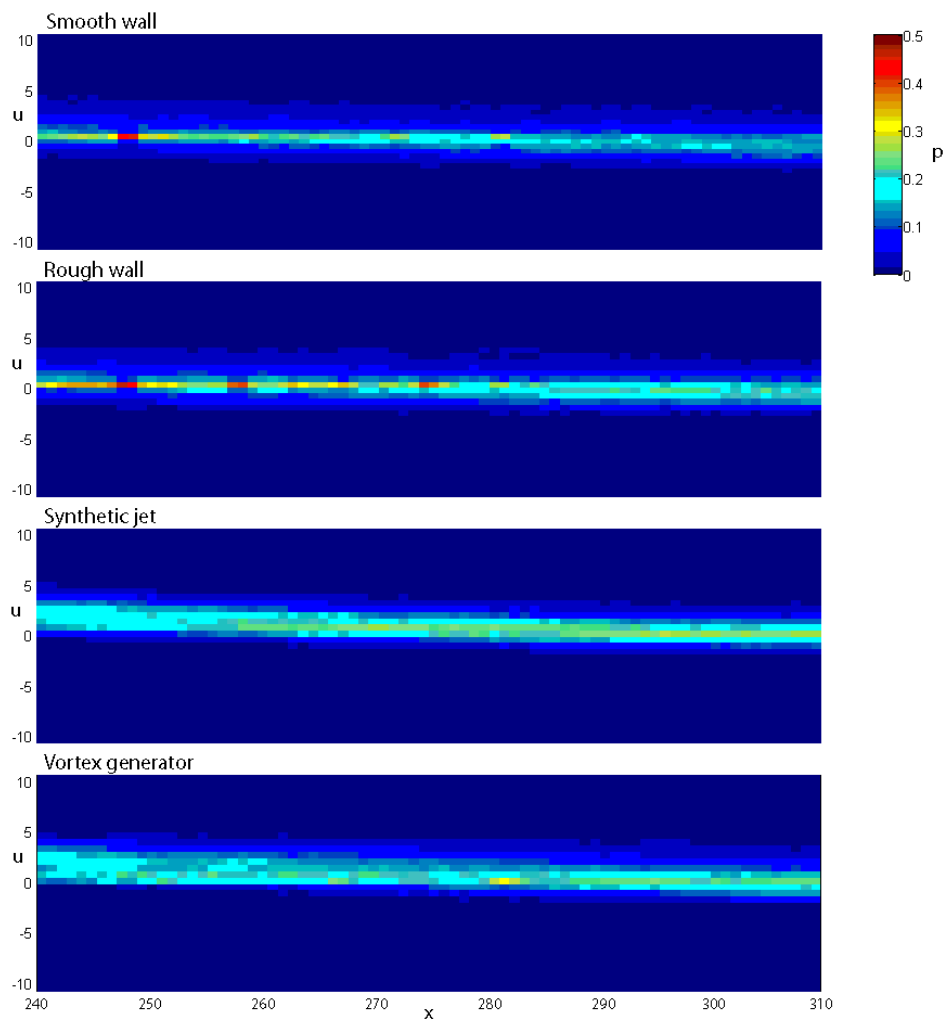


Fig. 19 – Histograms of instantaneous velocities near the wall

scales are logarithmic.

All spectra are characterized high values for low frequencies – order of 10 Hz, and decay for increasing frequencies. This tendency is explicit in Fig. 18. There are differences in values of maxims (e.g. for 10 Hz) as function of  $x$  position. While for smooth and rough wall we could see in Fig. 17 increasing value of spectrum with  $x$  position, for remaining two cases (synthetic jet and vortex generator) the tendency is just opposite. This is in accordance with findings given above, that the activity in separation region is for synthetic jet and vortex generator lower, than in the cases with smooth and rough wall. Please also note that in spectra of the longitudinal velocity component near the wall for the synthetic jet case, there is no peak in the synthetic jet excitation frequency 440 Hz.

To study velocity distribution near the wall we evaluated histograms of the instantaneous longitudinal velocity components  $u$  (vertical axis) for the given  $x$ -position (horizontal axis) – see Fig. 19. Color indicates probability density function distribution. The slight negative slope is evident for all distributions showing the tendency to appearance of negative instantaneous velocities  $u$  moving downstream. The first two cases (smooth and rough wall) show very sharp velocity distribution upstream the separation point indicating very moderate velocity fluctuations in this region. Distribution becomes much broader in the separation region. But then the last two cases (synthetic jet and vortex generator) show nearly constant shape of histograms independent on streamwise position (only mean value changes).

## Conclusions

The three variants of control strategies for a boundary layer separation were studied experimentally using the TR-PIV technique. The results show good ability of both synthetic jet and vortex generator to postpone the mean position of the separation point. Synthetic jet produces much more regular and steady behavior than the vortex generator. On the other hand, the traditional strategy using artificial wall roughness fails in control of already turbulent boundary layer.

The results are of qualitative nature, the individual control strategies could be optimized.

Of course, the flow in our relatively narrow channel is of 3D nature, especially near the side-walls. In the presented paper we studied only quasi-2D flow near the channel axis.

## Acknowledgement

The authors gratefully acknowledge financial support of the Grand Agency of the Academy of Sciences of the Czech Republic by the research project No. IAA2076403 and Grand Agency of the Czech Republic No. 101/05/0675.

## References

CHEN, F.-J., 2002. *Optimized Synthetic Jet Actuators*. LAR 16234, NASA Tech Briefs, July 2002.

---

KNOB, M., URUBA, V., 2007. *A Brief Survey of Vortex Identification Methods with Application to 2D*. 21st SYMPOSIUM ON ANEMOMETRY, PROCEEDINGS. Eds.: Chára, Klaboč, Praha, Institute of Hydrodynamics ASCR, v.v.i., pp. 75-80.

URUBA, V., JONÁŠ, P., MAZUR, O., 2007. *Control of a Channel-Flow Behind a Backward-Facing Step by Suction/Blowing*. International Journal of Heat and Fluid Flow. Volume 28, Issue 4, pp. 665-672.

URUBA, V., KNOB, M., POPELKA, L., 2007. *A Boundary Layer Separation Dynamics*. Engineering Mechanics 2007, book of extended abstracts. Ed.: Zolotarev, Praha, Institute of Thermomechanics AS CR, v.v.i., pp. 297-298.

URUBA, V., KNOB, M., 2007. *Application of TR-PIV Method to Turbulent Flow-Fields Studies*. 21st SYMPOSIUM ON ANEMOMETRY, PROCEEDINGS. Eds.: Chára, Klaboč, Praha, Institute of Hydrodynamics ASCR, v.v.i., pp. 163-170.

URUBA, V., KNOB, M., POPELKA, L., 2007. *Control Strategies for Boundary Layer Separation*. XXVI. Setkání kateder mechaniky tekutin, Herbertov, August 28 - 31, pp.93-94.

URUBA, V., 2004, *Synthetic Jet Actuator Design*. In: Proceedings of Topical Problems of Fluid Mechanics 2004, February 25, 2004, Prague, pp.169-174.